[논 문] 한국재료학회지
Korean J. Mater. Res.
Vol. 31, No. 3 (2021)

https://doi.org/10.3740/MRSK.2021.31.3.122

Effect of Silane Coupling Treatment on the Joining and Sealing Performance between Polymer and Anodized Aluminum Alloy

Sung-Hyung Lee[1,2,4†], Hitoshi Yashiro[2] and Song-Zhu Kure-Chu[3]

[1]Gakkō hōjin Kitahara gakuen, Hirakawa 036-0146, Japan
[2]Department of Chemistry and Biological Science, Iwate University, Morioka, Iwate 020-8551, Japan
[3]Materials Function and Design, Nagoya Institute of Technology, Nagoya, Aichi 466-855, Japan
[4]Shakai fukushi hojin wayo-kai, Hirakawa 036-0146, Japan

(Received November 9, 2020 : Revised February 16, 2021 : Accepted February 22, 2021)

Abstract In the fabrication of joined materials between anodized aluminum alloy and polymer, the performance of the metal-polymer joining is greatly influenced by the chemical properties of the oxide film. In a previous study, the dependence of physical joining strength on the thickness, structure, pore formation, and surface roughness of films formed on aluminum alloys is investigated. In this study, we investigated the effect of silane coupling treatment on the joining strength and sealing performance between aluminum alloy and polymer. After a two-step anodization process with additional treatment by silane, the oxide film with chemically modified nanostructure is strongly bonded to the polymer through physical and chemical reactions. More specifically, after the two-step anodization with silane treatment, the oxide film has a three-dimensional (3D) nanostructure and the silane components are present in combination with hydroxyl groups up to a depth of 150 nm. Accordingly, the joining strength between the polymer and aluminum alloy increases from 29 to 35 MPa, and the helium leak performance increases from 10^{-2}-10^{-4} to 10^{-8}-10^{-9} Pa m^3 s^{-1}.

Key words silane coupling agent, porous oxide film, joining strength, helium leak, waterproof.

1. Introduction

In recent years, there has been an increasing demand for lightweight materials having excellent strength for use in mobile electronic devices, lightweight automobiles, and industrial applications.[1,2] High-strength and lightweight components are considered one of the most efficient ways to save resources and energy. Metal-polymer joint parts, which are representative of high-strength and lightweight materials, are attractive also in chemical stability, flexibility, easy processing, and low cost. Therefore, there is increasing interest in the application of metal-polymer joining materials to various fields such as automotive parts, electronic parts and medical devices. As a result, studies on implementation of metal-polymer joining materials are actively being conducted.[3,4] Although laser or friction welding and ultrasonic bonding techniques have been investigated for fabrication of metal-polymer joint parts using injection technology, they generally do not have enough bonding strength for practical applications.[5-10]

With regard to the joining properties of polymers and metals, the chemical state of the metal surface is also an important factor. Izadi et al.[11] proved that the isocyanate group (NCO) introduced by toluene diisocyanate can significantly affect the joining strength between the polyamide 66 and the steel interface. In addition, an environmentally friendly and inexpensive silane coupling agent is used to combine organic and inorganic materials to form chemical bonds between them.[12] Moreover, the surface structure and composition of metals and polymers can be changed simultaneously to induce mechanical and chemical bonds at the bonding interface.[13] According to their results, the adhesive strength increases with increasing hydroxyl concentration at the Al (oxide) surface. All of these results proved that the anodizing method was very

†Corresponding author
E-Mail : shlee.sato@wayokai.jp (S.-H. Lee, Iwate Univ.)

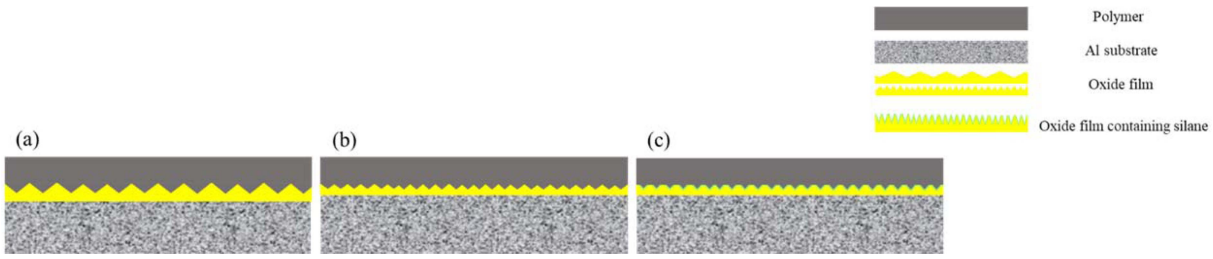

Fig. 1. Comparison of joining techniques. (a) anodizing, (b) two-step anodizing, (c) two-step anodization containing silane.

effective in improving the bond strength between the metal and polymer materials.[14)]

Fig. 1 shows three concepts of bonding between metal and polymer by general anodizing, two-step anodizing, and two-step anodizing modified with a silane coupling agent. Our previous study proved that the two-step anodizing method greatly improved the bonding strength with the polymer compared to the general anodizing method by minimizing the change in the roughness of the raw material while maximizing the surface area to be bonded by the anchor effect.[1)] However, the best reliability of waterproof performance cannot be achieved by physical bonding alone. To respond to current industry-issued electric vehicle battery packs and smartphones, it must meet dust and water resistance rating Ingress Protection (IP) 67. The second number, 7, denotes a waterproof rating. This requires a level where water does not damage the internal electronics when the product is left in 1M deep water for 30 min.

Therefore, in this study, the two-step anodized film was modified with a silane coupling agent to maximize physical and chemical bonds and the structural properties between metals and polymers were investigated. In addition, waterproof performance was evaluated using helium leak measurement technology.

2. Experimental Methods

The anodizing system consists of electrolytic components, high voltage supply, high current pulse reverse rectifier (NF, BP4650), stainless steel (type 316) heat exchanger and bubble installation. The experimental setup was described in ref. 1). Al-7075 alloy specimen with chemical composition and properties shown in Tables 1 and 2 were used as an anode (3 mm thick, 12 × 40 mm) as shown in Fig. 3, and graphite plates were used as a cathode.

It has been reported that fine porous alumina films can be prepared by the two-step anodization; electrochemically anodizing aluminum under certain conditions, followed by selective removal of the aluminum oxide produced and secondary anodization.[15)] The two-step anodizing process was performed as shown in Table 3 and the detailed condition was described in ref. 1).

In addition, in this study, silane coupling agent treatment and curing process were added as special treatments, and the coupling agent was dissolved in a solvent, and the volume ratios were 7 % and 30 %, respectively. γ-amino propyltriethoxy silane was used as a coupling agent for polymers and metals. The silane structure is given below:

$(CH_3\text{-}CH_2\text{-}O)_3SiCH_2CH_2CH_2\text{-}NH_2$

Hydrolysis and condensation reaction of the silane coupling agent are expected as shown in Fig. 2. Two-step anodized sample was immersed in the coupling agent solution for 3 min at a temperature of 30 °C. The excess solution was removed by air spray and then, was cured in an oven at 80 °C for 10 min to form a coupling agent film on the sample surface.

Metal and polymer-bonded specimens were prepared by the molding process described in Fig. 4, and the

Table 1. Chemical composition of tested 7075 aluminum alloy (wt %).

Al 7075	Si	Fe	Cu	Mn	Mg	Cr	Zn	Zr + Ti	Al
%	0.40	0.50	1.2 ~ 2.0	0.30	2.1 ~ 2.9	0.18 ~ 0.35	5.1 ~ 6.1	0.25	Bal.

Table 2. Mechanical properties of material.

Material	Tensile strength (Mpa)	Melt temperature (°C)	Heat distortion temperature (°C)	Density (g/cm^3)	Elongation at rupture (%)
PPS	170	310	140	1.57	2
Al 7075	510	483	/	2.80	17

Table 3. Flow chart of two-step anodization process with silane.

Process	Bath composition	Temp (°C)	Time (Min)	Current density, i/(A dm^{-2})
Degreasing	1 % Surfactants	50	3	-
Etching	2 % NaOH	50	1	-
Activation	1 % H_2SO_4	30	1	-
1st anodization	2 % $C_2H_2O_4$ 0.5 % MH_3PO_4	70	15	2
Remove the 1st anodizing film	1 % H_2SO_4	30	0.5	-
2nd anodization	2 % $C_2H_2O_4$ 0.5 % $C_3H_8O_3$	70	15	0.5
Coupling agent mixture	7 % Coupling agent 30 % Solvent	30	3	-
Curing	-	80	10	-

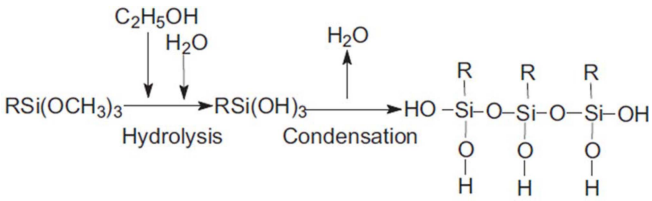

Fig. 2. Hydrolysis of γ-aminopropyltriethoxy silane.

structure of the finished specimen is illustrated in Fig. 3(b). Polypropylene sulfide (PPS) with 30 % (wt) glass fiber from Polyplastics Co., Ltd. of Japan was used as a polymer material. The applied DURAFIDE 1130A1 type

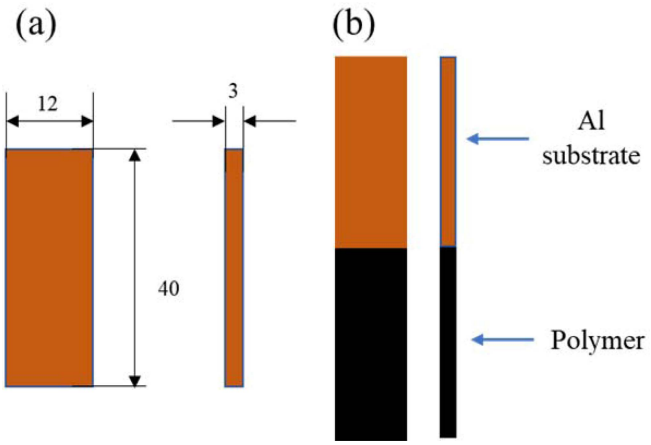

Fig. 3. Structure of test specimens (a) Metal specimen, and (b) Al - polymer joining specimen for tensile test.

is characterized by high stiffness and strength, good dimensional stability, chemical resistance and heat resistance. The PPS resin was dried at 140 °C for 4 h before the injection process. The main properties of PPS materials are summarized in Table 2.[1] The injection parameters used in the molding process are presented in the previous study.[1] In addition, joining strength tests of metals and polymers were performed.

Finally, a helium leak test was conducted to verify waterproofness. In this study, ULVAC's HELiOT 900 was used, with a structure of the test specimen shown in Fig. 5(a). Helium leak rate was measured using the vacuum spray method described in Fig. 5(b).

The surface and cross-section of the anodized sample

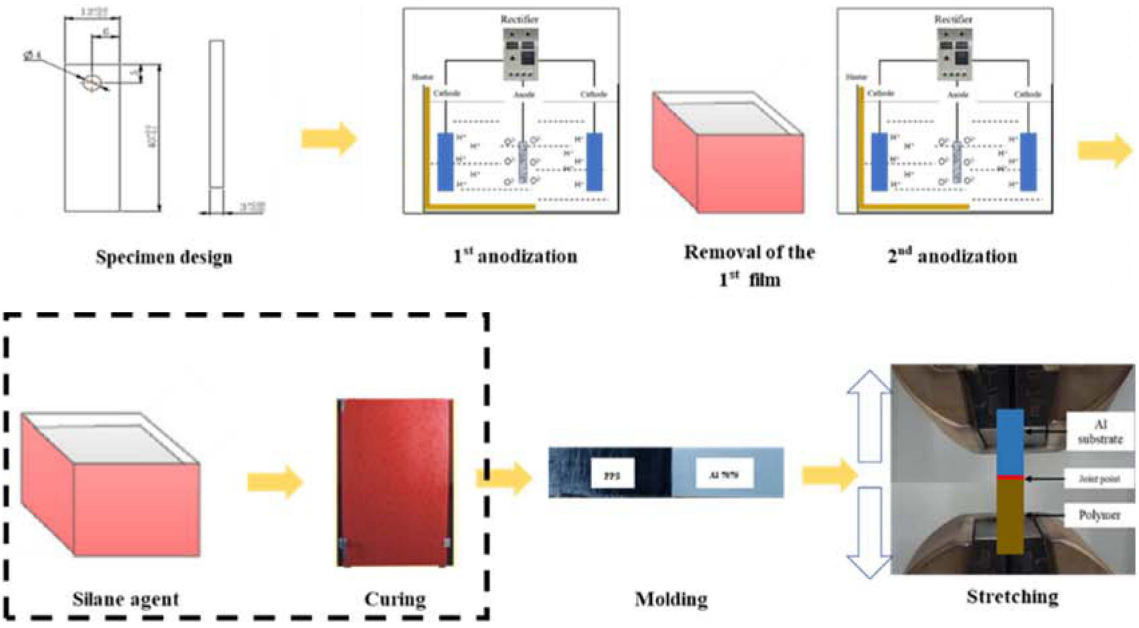

Fig. 4. Schematic diagram of injection molding process for the manufacture of joining material of Al alloy and polymer.

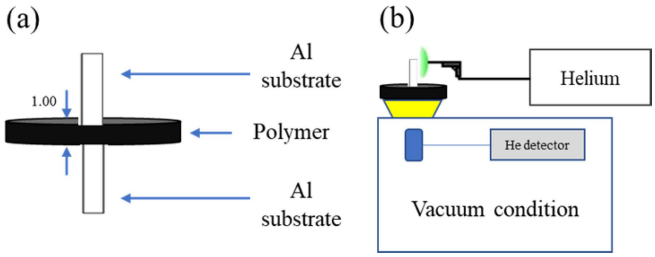

Fig. 5. Structure of test specimens (a) He leak test, (b) helium leak tester.

was examined using a field emission scanning electron microscope (FESEM). The specimen was cut, cooled and polished with silicon carbide (SiC) paper, and the composition of the oxide layer was analyzed using EDS. The texture and crystal structures of the as-anodized specimens formed in different electrolytes were observed using a transmission electron microscope (TEM: JEOL-JEM-2100, 200 kV). The specimen for TEM observation was prepared using focused ion beam (FIB) after C and Pt protective layers were deposited onto the film surface via vacuum evaporation. Here, the reason that interlayer C was coated prior to Pt layer is to avoid Pt particles entering the nanopores, which may affect the SAED patterns.

The composition and chemical states of the porous alumina films were analyzed by X-ray photoelectron spectroscopy (XPS: ULVACPHI-5600CIM, Mg Kα), using a five channel analyzer (VG Scientific ESCALAB 200-X) in an operating vacuum better than 1×10^{-9} Torr (1 Torr ≅ 133 Pa). The binding energies of the spectra were corrected using the C1s signal at 284.5 eV, with an accuracy of less than 0.1 eV. Moreover, the depth distributions of elements in the as-anodized specimens were investigated by glow discharge optical emission spectrometry (GDOES: HORIBA-JY-5000RF, 4 mm diameter, 13.56 MHz, 35 W, Ar-600 Pa). Fourier transform infrared spectroscopy (FTIR) was collected (as KBr-pressed pellets) on a Nicolet 170SX FT-IR spectrophotometer in the range of 400 ~ 5000 cm^{-1}.

The bond strength of metal and polymer was measured by a precision tester (SSTS, CMT 4204) with a head speed of 1.0 mm min^{-1}.

At least, three specimens of each case were tested to ensure reliability of tests results.

3. Results and Discussion

Fig. 6 shows schematics of the joining images between polymer chain and aluminum alloy surface formed by the three types of treatments: anodizing, two-step anodizing and two-step anodizing with silane-treatment. In Fig. 6(a), a porous oxide film with hydroxyl groups is formed on the aluminum surface, and it turns to a film with a 3D nanostructure after the two-step anodization with increased surface area. A relatively large amount of hydroxyl groups is produced in Fig. 6(b). In Fig. 6(c), silane coupling and curing treatments are added after the two-step anodization treatment according to the processes of Fig. 4 and Table 3. The oxide film on the anodized Al alloy provides a fine structure with hydroxyl groups suitable for improving the physical and chemical intercalation through coupling agent.[14] Hydroxyl groups can react with the coupling agent to form Al-O-Si bonds, which enhance the combination of the coupling agent and aluminum hydroxide through chemical interactions. The alkoxysilyl group of the silane coupling agent is hydrolyzed to form silanol, which condenses with the metal hydroxide surface to form a Si-O-M bond.[15] In addition, the amino group at the end of the silane coupling agent acts to increase adhesion through chemical or physical entanglement with the polymer chain.

Fig. 7 shows the schematic illustration of the formation of Al-O-Si bonding inside the nanopore after the silane coupling treatment. In addition, in the two-step anodization

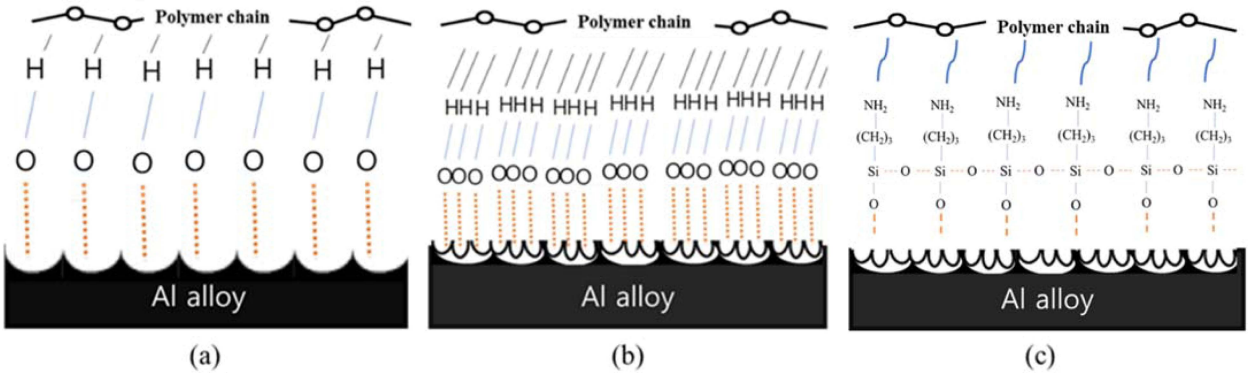

Fig. 6. Joining images between polymer chain and aluminum alloy surface treated by (a) 1st anodization, (b) 2nd anodization, and (c) 2nd anodization + silane coupling agent.

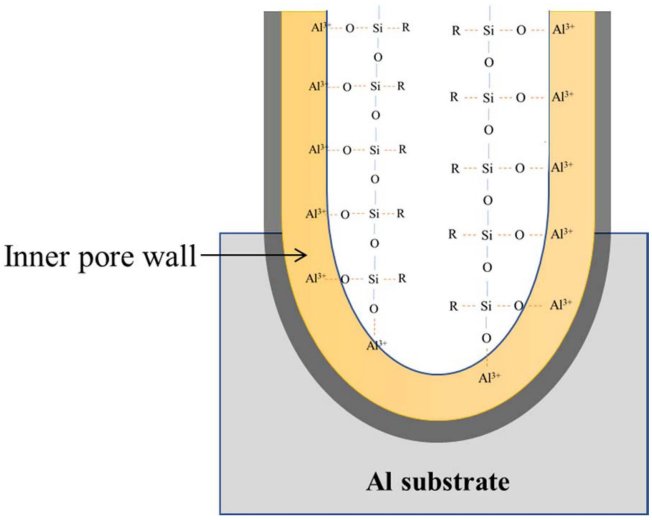

Fig. 7. Schematic illustration of the formation Al - O - Si bonding on the inner walls of the nanopore after the two-step anodization followed by silane treatment.

process containing silane, an Al-O-Si bonding structure is formed on the inner pore wall. In a two-step anodization process including silane treatment, FTIR spectrum analysis was performed to detect chemical changes on the surface of the oxide film.

Fig. 8 shows the FTIR spectrum of the untreated raw material and silane-treated aluminum material after anodization. In the case of the untreated raw material, a broad peak appeared in the region of Al_2O_3 (1,000 ~ 400 cm^{-1}) due to the presence of a natural oxide film generated in the atmosphere due to the properties of the aluminum. In the case of the specimen treated with anodization, silane-treatment, and curing, a stretching vibration peak of Al_2O_3 (848 cm^{-1}) and broad one of OH (3,400 cm^{-1}) appeared. They originate from anodizing process. The Si-O (1,070 cm^{-1}) peak which appeared after the silane-treatment confirmed the formation of the γ-aminopropyltriethoxy silane organic coating film on the surface of the aluminum alloy specimen, The peak of C=O (1,700 cm^{-1}) stretching vibration of C-O group is ascribed to oxalic acid and glycerol from electrolyte, and a weak band peak at 1,647 cm^{-1} to water.

Fig. 9 shows the fine surface and cross section of the oxide film formed by two-step anodization including silane process. The conditions for the electrolyte and silane treatment and curing processes are given in Table 3. Fig. 9(a) indicates that the pore width of the anodized and silane-treated sample surface was 10 ~ 35 nm, and the outermost layer of the high-purity ceramic pore wall formed in the first step anodizing remained in the form of hair forming a 3D nanostructure pores. In the anodizing process, the pores become more pronounced in a high temperature electrolyte because of high solubility of metal.[16] In addition, the porosity of the oxide film increased as the purity of the Al material decreased.[17] Fig. 9(b) shows the cross-section and thickness of the anodized oxide film with silane-treatment. It represents the three-layer structure of the two-step anodized film, and the silane is contained in the outermost layer having a thickness of about 100 nm. The total thickness of the oxide film is 200 ~ 250 nm. It is reported that the alignment mechanism of the pores is caused by the mechanical force due to the volume change that occurs when aluminum is converted to alumina.[18] The thickness

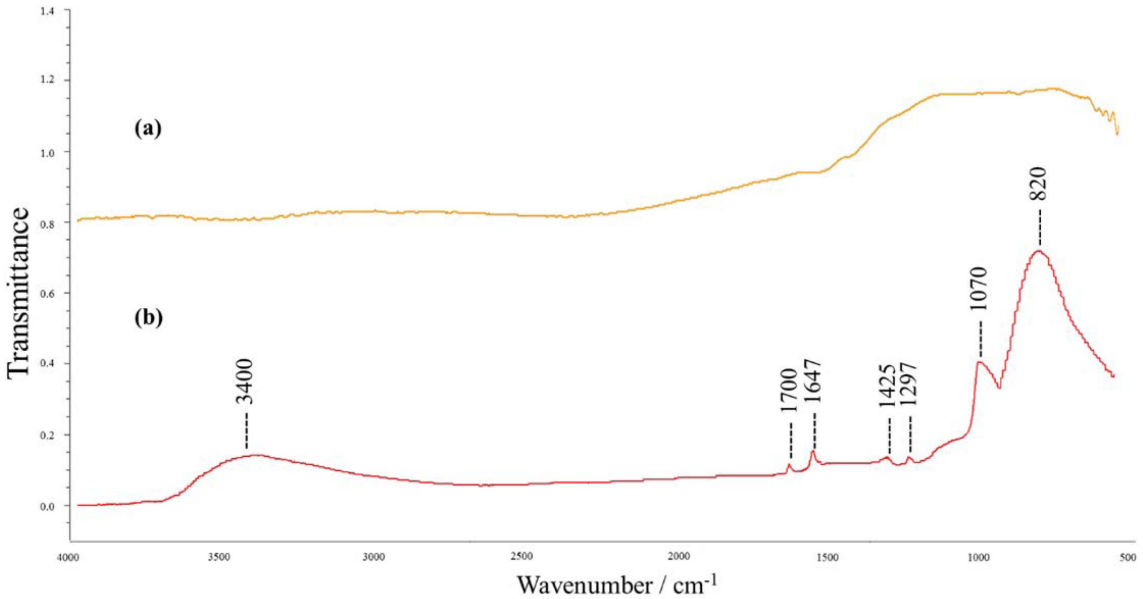

Fig. 8. Fourier transform infrared spectra of the specimens (a) before and (b) after 2nd anodization + silane treatment.

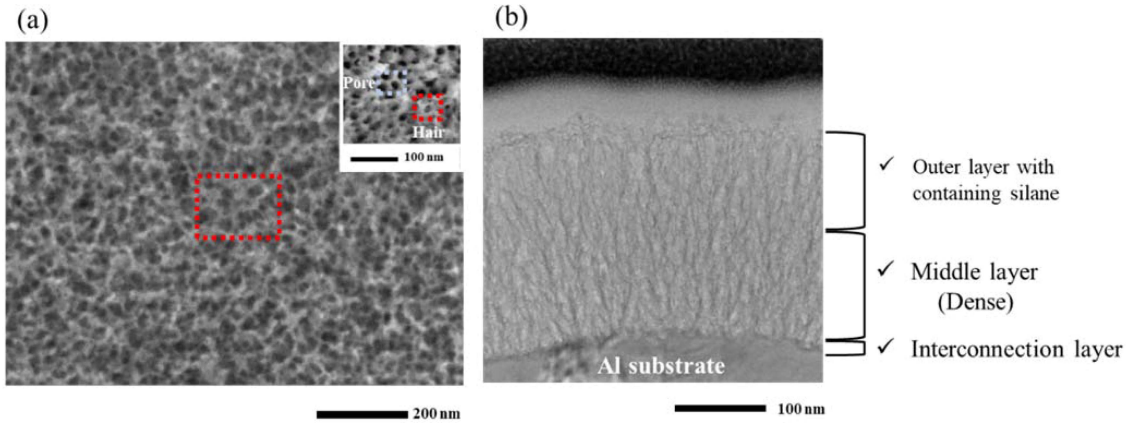

Fig. 9. (a) Surface morphologies and (b) cross-sectional view of the specimen after the two-step anodization and silane treatment.

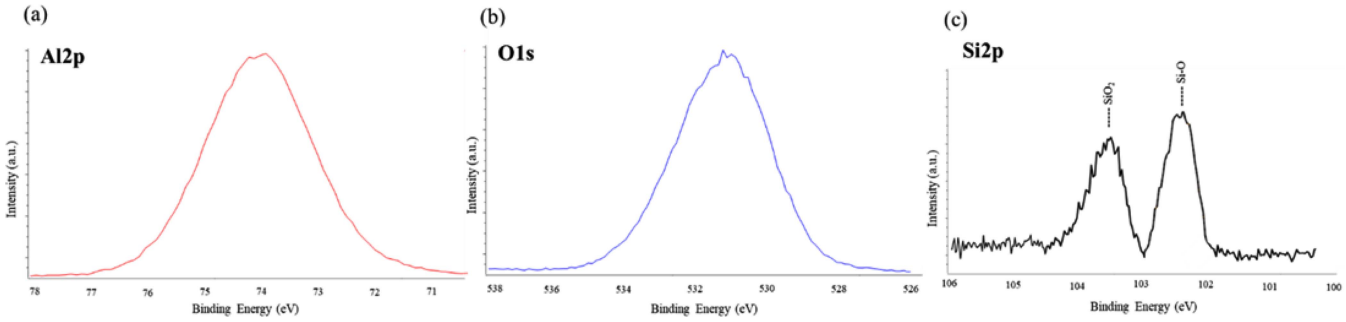

Fig. 10. XPS spectra of the specimen after the two-step anodization and silane treatment.

of the barrier layer generally corresponds to an applied voltage along 1.2 nm/V.[19)]

In addition, the formation of alumina during anode oxidation is accompanied by dissolution of impurities (i.e., Fe, Cu, Zn, Mg, Mn, etc.) according to the following reactions.

$$2Al + 3H_2O \rightarrow Al_2O_3 + 6H^+ + 6e^- \quad (1)$$

$$M \rightarrow M^{n+} + ne^- \ (M = Fe, Cu, Zn, Mg, Mn, etc.) \quad (2)$$

The XPS spectra of the oxide film after the two-step anodization and silane coupling treatment are shown in Fig. 10. Typical spectra of O1s and Al2p for aluminum oxide were confirmed. In addition, Si2p spectrum was assigned to SiO_2 from alloy substrate and Si-O from the silane. Aluminum is present mainly in the form of γ-Al_2O_3 and Al $(OH)_3$ bayerite before anodizing, and in the form of AlO(OH) and $Al(OH)_3$ after anodizing. Therefore, the anodized Al surface contains relatively more hydroxyl groups. In addition, since the affinity of AlO(OH) for the silane coupling agent is relatively better than that of Al_2O_3, these properties make the reaction between the hydroxyl group and the oxide film present in the coupling agent much easier.[20)]

Fig. 11 shows the depth profile of the atomic fraction of Si in the form of SiO_2 and Si-O (silane). The sputtering rate of the film was calculated with reference to the thickness (about 250 nm) in Fig. 9(b). From the XPS depth profile, Si-O derived from the silane coupling agent was detected to a depth of 0 ~ 150 nm of the oxide film, and SiO_2 derived from the oxide film was detected in the entire layer of the oxide film. As a result, it was confirmed that the silane coupling agent was concentrated and distributed in the outer layer of the oxide film (See Fig. 9(b)).

Fig. 12 shows a cross-sectional TEM image of the oxide and polymer interface from the Al-PPS joining specimen formed according to the process sequence of Fig. 4. To investigate the interfacial area where the aluminum alloy and polymer were jointed, a lamellar was prepared using focused ion beam (FIB) milling from the cross section of the sample, and the cross section was measured using a high resolution TEM. The porous 3D nanostructure and three-layer structure of the oxide film observed in previous studies were confirmed, and the porous outer layer has a thin hair structure that contributes to strong adhesion to the polymer.[1)] It was also confirmed that the outer layer containing silane was jointed to the polymer [See Figs. 9(b), 11]. When a high

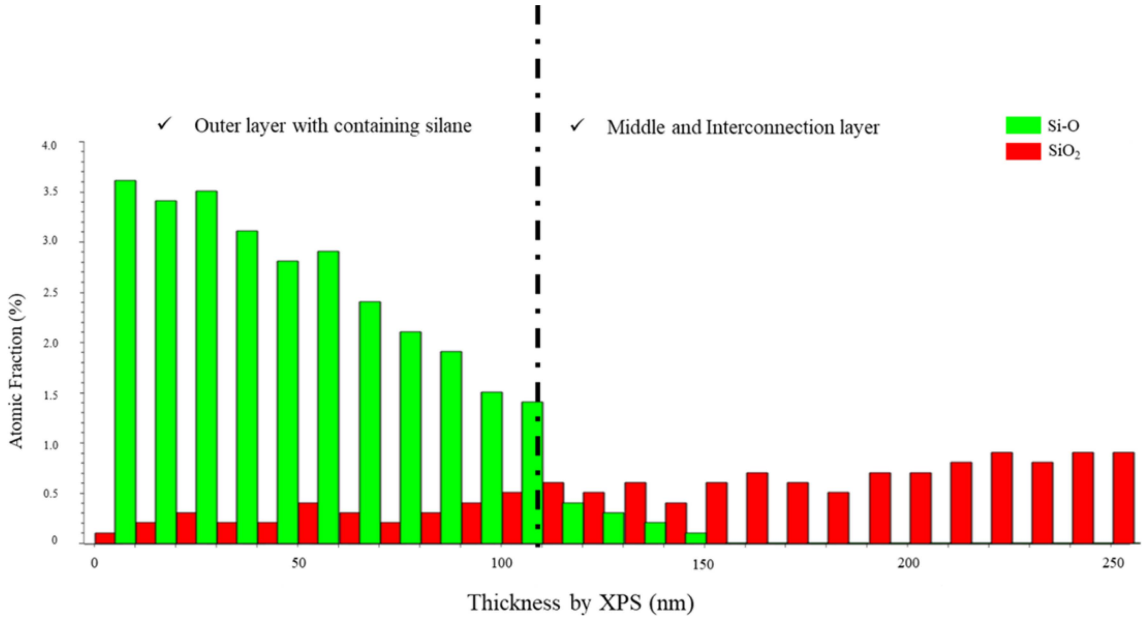

Fig. 11. XPS depth profile of SiO_2 and Si-O content after two-step anodization and silane coupling agent treatment.

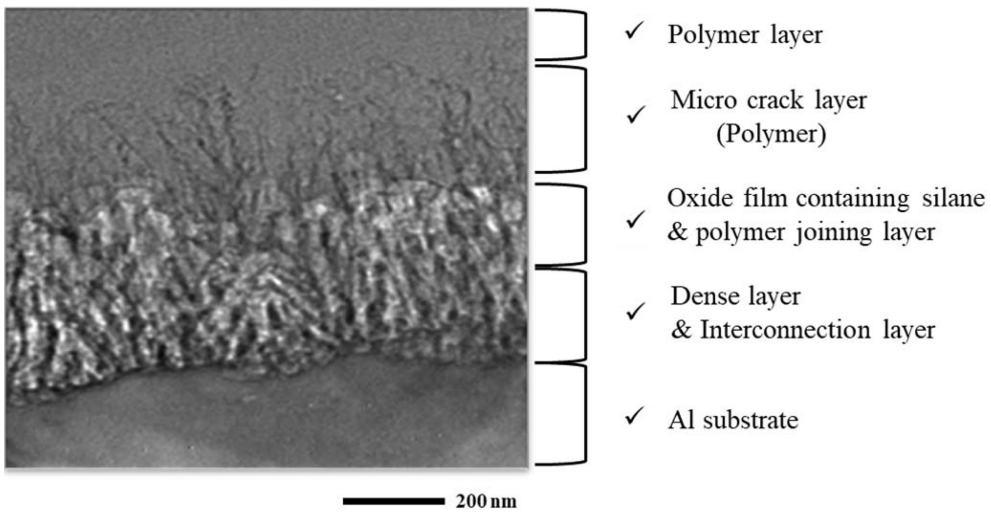

Fig. 12. Cross-sectional view of the joining interface between aluminum alloy and polymer with two-step anodizing and silane coupling treatment.

temperature electrolyte is used, the outer pores of the oxide film tend to be widened by chemical dissolution. The widened pores through chemical dissolution facilitate contact with the polymer and aid in penetration into the pores. In addition, a large amount of cracks were formed in the vertical direction in the polymer at the interface jointed to the outer layer of the oxide film. They probably formed when the polymer is filled into the pores of the oxide film.

Fig. 13 shows the distribution of elements determined by energy dispersive X-ray spectroscopy (EDS) over the cross-section of the boundary between the polymer and the Al alloy. C, Si and S detected in the polymer and micro-crack layer are the main components of the polymer. In the outer layer, Al, O, C and Si, the main components of the oxide film and polymer, were detected, and the concentration of Si was relatively increased compared to the polymer and micro crack layers. As the cause of Si in the outer layer of oxide film, the glass fiber in the polymer SiO_2 from the Al 7075 material and Si-O components from the silane coupling agent can be counted.

Fig. 14 shows the joint strength between the polymer and the aluminum alloy joined after the two-step anodizing and silane treatment. As a result, the silane treatment increased the averaged joining strengths from

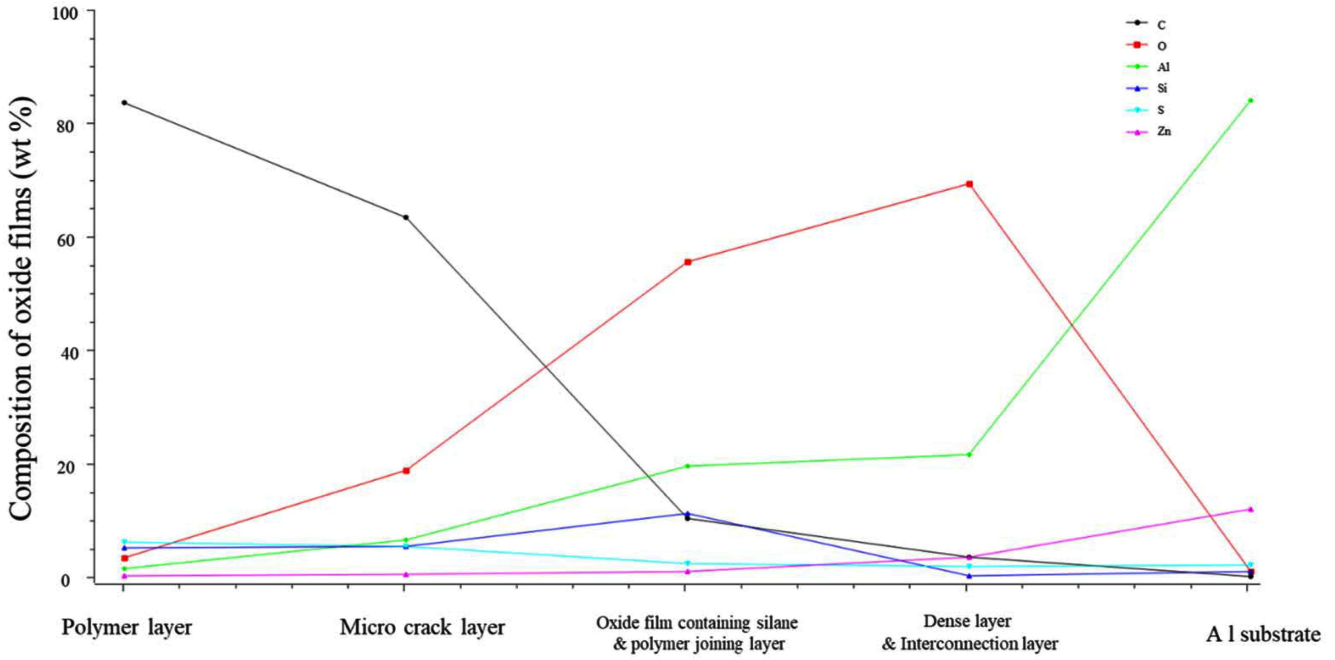

Fig. 13. EDS analysis of the joining interface between aluminum alloys and polymers using two step anodizing and silane coupling treatment.

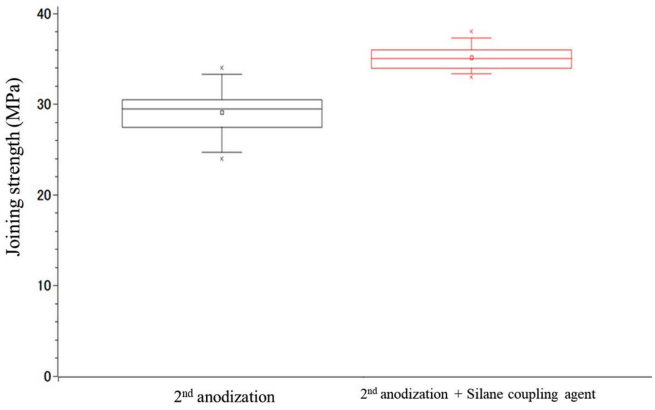

Fig. 14. Improvement of joining strength between Al-7075 alloy and PPS polymer by the two-step anodization.

29 MPa to 35 MPa.

Fig. 15 shows the fracture surfaces after the tensile testing. As shown in Fig. 15(b-1) and (b-2), the fracture interface indicated higher joining strength of specimen with the two-step anodization process including (b-2) silane. The chemical composition of the fractured interface analyzed by EDS is shown in Fig. 15(c). Under both conditions, Al, O, the main component of the oxide film, and C, the main component of the polymer, were detected. The product treated under the two-step anodization condition had a relatively high content of Al, the main component of aluminum metal. In addition, under the two-step anodization conditions including silane, the concentrations of O, C as the main components of the oxide film and the polymer, and Si as the main components of the silane were relatively high. It was confirmed that an oxide film containing silane was present together with polymer component.

Fig. 16 shows that the helium leak performance was much improved by the silane treatment. The experimental results showed that permeation rate ranged from 10^{-2} to 10^{-4} Pa m^3 s^{-1} and 10^{-8} to 10^{-9} Pa m^3 s^{-1} for the specimens with the two-step anodizing and with subsequent silane treatment, respectively. As a result, the performance in the range of 10^{-8} to 10^{-9} Pa m^3 s^{-1} for the silane treated specimen is a level that satisfies the dustproof and waterproof grade IP 67 of the smartphone. It is also capable of satisfying the quality standards of lithium ion batteries for electric vehicles used in much harsher environments. In the case of lithium-ion battery cells of electric vehicles, strict quality standards are applied because it can cause fire in case of leakage of the electrolyte inside. The difference in these results is caused by the strong interaction between the oxide film and the polymer due to the physical and chemical forces generated by the porous 3D nanostructure oxide film and silane coupling.

The two-step anodization technique further improved by the silane treatment proposed in this study is advantageous for mass production and is useful for manufacturing composites of metals and polymers with complex structures.

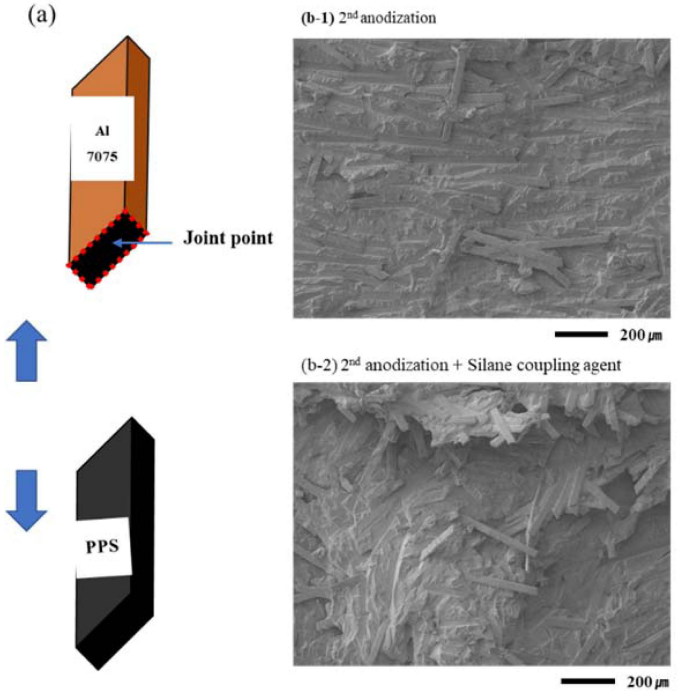

(c)

Element	Mass (%)	
	(b-1)	(b-2)
Al	52.1	2.8
O	11.8	27.9
C	28.3	58.5
Si	7.8	10.8

Fig. 15. Fracture surface after tensile test. (a) Al-PPS structure, (b) Surface of joint point, (c) EDS analysis data.

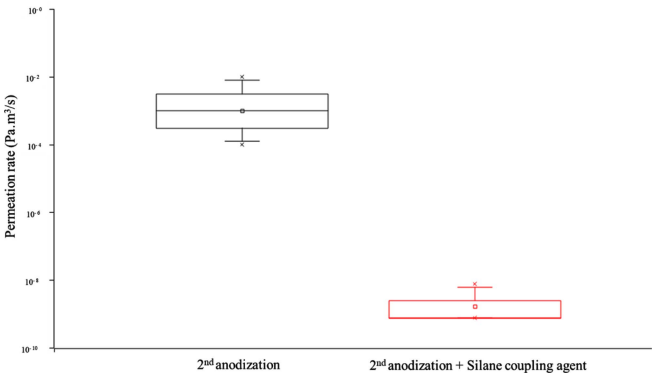

Fig. 16. Evaluation of helium leak test.

4. Conclusions

We have described the anodization technology that includes a silane treatment step which is effective for the production of joining materials of Al alloys with polymers with waterproof and sealing properties that are applicable to lithium-ion batteries and smartphones in electric vehicles. The two-step anodizing process proposed in the previous study has strong joining force but is inadequate in term of waterproofness and sealing force. In this study, a process of forming an oxide film having strong waterproofing, sealing, and joining properties by penetrating silane into the outer layer pores of the 3D nano-structured oxide film is optimized. After the two-step anodization including silane treatment, the tensile force, waterproofing and sealing force were significantly improved compared to the case without silane treatment. By the introduction of silane into the outer layer of 150 nm of the oxide film, the joining strength of Al alloy and polymer increased from 29 to 35 MPa, and the helium leak performance increased from $10^{-2} \sim 10^{-4}$ to $10^{-8} \sim 10^{-9}$ Pa m^3 s^{-1}. Maximum interfacial joining strength and sealing performance were obtained by physical and chemical joining of Al alloy and polymer by the two-step anodizing process with an optimized silane treatment.

This technology can be applied to the manufacture of high-performance composite structures in various fields including lithium-ion batteries and smart phone parts of electric vehicles that require high reliability and waterproofing.

References

1. S. H. Lee, H. Yashiro and S. Z. Kure-Chu, J. Korean Inst. Surf. Eng., **53**, 144 (2020).
2. S. H. Lee, H. Yashiro and S. Z. Kure-Chu, Korean J. Mater. Res., **29**, 288 (2019).
3. N. Z. Borba, L. Blaga, J. F. dos Santos and S. T. Amancio-Filho, Mater. Lett., **215**, 31 (2018).
4. Y. Kajihara, Y. Tamura, F. Kimura, G. Suzuki, N. Nakura and E. Yamaguchi, CIRP Annals, **67**, 591 (2018).
5. D. Quan, N. Murphy and A. Ivankovic, Int. J. Adhes. Adhes., **77**, 138 (2017).
6. Y. J. Chen, T. M. Yue and Z. N. Guo, J. Mater. Process.

Technol., **249**, 441 (2017).
7. E. E. Feistauer, R. P. M. Guimaraes, T. Ebel, J. F. D. Santos and S. T. Amancio-Filhoac, Mater. Lett., **170**, 1 (2016).
8. A. J. Al-Obaidi, Ph. D. Thesis, p.1-246, University of Sheffield (2018).
9. F. Lambiase, A. Paoletti, V. Grossi and S. Genna, J. Mater. Process. Technol., **250**, 379 (2017).
10. F. Lambiase and S. Genna, Int. J. Adhes. Adhes., **84**, 265 (2018).
11. O. Izadi, P. Mosaddegh, M. Silani and M. Dinari, J. Manuf. Process., **30**, 217 (2017).
12. A. B. Abibe, M. Sonego, J. F. D. Santos, L. B. Canto and S. T. Amancio-Filho, Mater. Des., **92**, 632 (2016).
13. F. C. Liu, J. Liao, Y. Gao and K. Nakata, Sci. Technol. Welding and Joining, **20**, 291 (2015).
14. S. T. Abrahami, T. Hauffman, J. M. M. D. Kok, J. M. C. Mol and H. Terryn, J. Phys. Chem. C, **120**, 19670 (2016).
15. Y. Xie, C. A. S. Hill, Z. Xiao, H. Militz and C. Mai, Compos. Part A: Appl. Sci. Manuf., **41**, 806 (2010).
16. H. Masuda and K. Fukuda, Science, **268**, 1466 (1995).
17. S.-Z. Kure-Chu, K. Osaka, H. Yashiro, H. Segawa, K. Wada and S. Inoue, J. Electrochem. Soc., **162**, C24 (2015).
18. O. Jessensky, F. Muller and U. Gosele, Appl. Phys. Lett., **72**, 1173 (1998).
19. S. T. Abrahami, Ph. D. Thesis. Delft University of Technology (2016).
20. B. Arkles, Silane coupling agents: connecting across boundaries, p. 9, Morrisville (2003).

Author Information

Sung-Hyung Lee
Gakkō hōjin Kitahara gakuen, Director
Shakai fukushi hōjin wayō-kai, Director
Iwate University yashiro ken research group, Special Researcher

Hitoshi Yashiro
Iwate University, Professor

Song-Zhu Kure-Chu
Nagoya Institute of Technology, Professor